

Mediterranean Marine Science

Vol 15, No 2 (2014)



Ecosystem dynamics in the Liguro-Provençal Basin: the role of eddies in the biological production.

E. CASELLA, P. TEPSICH, X. COUVELARD, R.M.A. CALDEIRA, K. SCHROEDER

doi: [10.12681/mms.520](https://doi.org/10.12681/mms.520)

To cite this article:

CASELLA, E., TEPSICH, P., COUVELARD, X., CALDEIRA, R., & SCHROEDER, K. (2014). Ecosystem dynamics in the Liguro-Provençal Basin: the role of eddies in the biological production. *Mediterranean Marine Science*, 15(2), 274–286. <https://doi.org/10.12681/mms.520>

Ecosystem dynamics in the Liguro-Provençal Basin: the role of eddies in the biological production

E. CASELLA^{1,2}, P. TEPSICH^{1,2}, X. COUVELARD³, R.M.A. CALDEIRA^{3,4} and K. SCHROEDER⁵

¹ CIMA Research Foundation, Via Armando Magliotto, 2 - 17100 Savona, Italy

² DIBRIS, University of Genoa, Via Opera Pia, 13 - 16126, Genova, Italy

³ CCM-Center for Mathematical Sciences, University of Madeira, Campus da Penteada, 9000-390, Funchal, Madeira, Portugal

⁴ CIIMAR-Interdisciplinary Centre of Marine and Environmental Research, Rua dos Bragas, 289, 4050 - 123 Porto, Portugal

⁵ CNR - ISMAR, Institute for Marine Science Arsenale - Tesa 104 Castello 2737/F 30122 Venezia, Italy

Corresponding author: elisa.casella@cimafoundation.org

Handling Editor: Elina Tragou

Received: 26 June 2013; Accepted: 22 January 2014; Published on line: 2 May 2014

Abstract

We studied, numerically, the role of mesoscale structures in the Ligurian Sea (NW Mediterranean Sea) as a possible factor affecting the spatial distribution of the chlorophyll spring bloom. We used the Regional Ocean Modelling System (ROMS) configured for the NW Mediterranean Sea (ROMS_NWMed) and satellite derived Altimetric, Sea Surface Temperature and Chlorophyll concentration data, for years 2009 and 2010. Comparison of model output with satellite and in situ data shows agreement between numerical results and observations. There is a significant interannual variability in concentration and distribution of chlorophyll in the basin during the two years of the study. The ROMS_NWMed simulation reveals the formation of a number of mesoscale eddies along the Northern rim current characterized by a long lifetime and closed streamlines. A significantly higher number of eddies was found during the chlorophyll-rich year 2010. The high number of eddies, due to the “eddy pumping mechanism”, generate spatially and temporally localised fluxes of nutrients into the euphotic zone, thus contributing to the fertilization of the Ligurian Sea. Therefore, eddies in the Ligurian rim current can have important effects on the location of development of the main patch of chlorophyll spring bloom and consequently on local ecosystem dynamics.

Keywords: Ocean model, Mesoscale eddies, Ligurian Sea, Spring bloom.

Introduction

The Liguro-Provençal Basin, North Western Mediterranean, is the main blooming area of the Mediterranean Sea (D’Ortenzio & d’Alcalà, 2009). Nevertheless, this region is known to be oligotrophic (Nezlin *et al.*, 2004; D’Ortenzio & d’Alcalà, 2009). Therefore, any supply of nutrients is extremely valuable to sustain the whole trophic chain. Oceanographic processes leading to the spring phytoplankton bloom in the area are largely driven by the main circulation. The regional hydrodynamics of the Liguro-Provençal Basin is dominated by a cyclonic circulation system. The Eastern Corsica Current (ECC) and the Western Corsica Current (WCC) feed this cyclonic circulation system, which is known as the Northern or Liguro-Provençal-Catalan Current. Differences in water density between the Northern Current and the central part of the basin generate a frontal zone that clearly separates coastal from open sea waters (Birol *et al.*, 2010; Poulain *et al.*, 2010). Moreover, sea level depression caused by cyclonic circulation leads to upwelling of nutrient-rich and

colder water, which consequently leads to phytoplankton blooms in the area.

This circulation pattern is persistent throughout the years, but it is affected by strong seasonality (Birol *et al.*, 2010; Picco *et al.*, 2010) reflected in the seasonal cycle of the biological production of the Ligurian Sea (Arnone, 1994). Strong spatio-temporal interannual changes of biological production have been observed and studied at basin (Estrada *et al.*, 1999; Barale *et al.*, 2008), regional (Estrada *et al.*, 1999; Nezlin *et al.*, 2004; Marty & Chiavérini, 2010) and local (Goffart *et al.*, 2002) scale. System heterogeneity is closely associated with local and regional hydrodynamic factors.

While flowing along the coastal slopes of Italy, France and Spain, the Northern Current is affected by instability processes. These processes generate (sub)mesoscale eddies, capable of inducing relatively intense shelf-edge flows, producing significant dynamic heterogeneity (Millot, 1991). The presence of these mesoscale eddies in the Western Mediterranean Sea is well documented (Santoleri *et al.*, 1983; Marullo *et al.*, 1985; Sammari *et al.*,

1995; Gasparini *et al.*, 1999; Robinson & Leslie, 2001; Echevin *et al.*, 2003), and it has been demonstrated that eddies can significantly affect the dynamics of the marine ecosystem (Jenkins, 1988; Falkowski *et al.*, 1991; McGillicuddy & Robinson, 1997; Abraham, 1998; Martin *et al.*, 2002; Lévy & Klein, 2004; Pasquero *et al.*, 2005). In particular, mesoscale and submesoscale vortices play a crucial role in determining transport processes and the statistical properties of the mesoscale turbulence field (Provenzale, 1999; Bracco *et al.*, 2000, 2003). In previous simulations of the Ligurian Sea, Casella *et al.* (2011) highlighted that mesoscale and submesoscale eddies are associated with strong vertical velocities, which generate significant upward and downward exchanges. This phenomenon can play an important role for the dynamics of marine ecosystems. Moreover, variations in the mixed layer depth (MLD) are usually associated with the presence of eddies. The MLD strongly influences biochemical cycles, with consequences on local productivity (Troupin *et al.*, 2010).

In the North Western Mediterranean Sea, the near shore zone is rich in eddies generated by the instabilities of the Northern Current. This is reflected in the high values of Eddy Kinetic Energy (EKE) in the coastal-rim area (Fig. 1). The peculiar feature of the North Western Mediterranean Sea is that, in contrast to many other marginal seas rich in mesoscale eddy activity, the near shore zone is poor in chlorophyll concentration (Nezlin *et al.*, 2004). The main primary production bloom occurs in the central part of the Liguro-Provençal basin, which is characterized by low values of EKE (Fig. 1) thus indicating less eddy activity.

In this paper, we investigate the role of the rim of eddies identified along the Liguro-Provençal current during the spring bloom of the Ligurian Sea. In particular, we focus on the hypothesis that the rim of eddies acts on the

containment of the bloom patch occurring in the central part of the basin and on the enrichment of nutrients in this basin and, as a consequence, eddies can represent one of the local factors responsible for the spatial variability of the bloom patch. For that purpose, the effect of eddies on the distribution of properties, their population distribution and their possible role as one of the local processes affecting the location of the main patch of chlorophyll in the study area has been analysed at different scales with data from remote sensing and an oceanic model.

The paper is organized as follows: section 2 presents the data and data analyses used, and also the detailed configuration of the ROMS model used for the NW Mediterranean Sea, including information on atmospheric and oceanic forcing. This section also contains a description of the eddies detection algorithm. Model validation and results of the analysis performed at different spatial scales (Large-, Regional- and Meso-scale) for the satellite and simulated data are presented in section 3. Discussion and conclusions are detailed in section 4.

Materials and Methods

Satellite products

The altimeter products used in this study were produced by Ssalto/Duacs and distributed by Aviso, with support from CNES (<http://www.aviso.oceanobs.com/duacs/>). In particular, we used the merged products of Absolute Dynamic Topography (ADT) and Sea Level Anomalies (SLA). ADT is obtained adding along track SLA to a mean dynamic topography (Rio & Hernandez, 2004). For the Mediterranean region, maps of ADT (MADT) and SLA (MSLA) are available with 8-day and $1/8^\circ$ temporal and spatial resolution respectively. MADT and MSLA gridded products are obtained by merging measurements from all available altimeter missions (Ducet *et al.*, 2000). It has in fact been demonstrated that combining data from different missions significantly improves the estimation of mesoscale signals (Pascual *et al.*, 2006). Furthermore, our study period (2009-2010) has one of the best altimetric coverage with a four-satellite constellation (Jason 1, Jason 2, Envisat and Cryosat). We used geostrophic velocities provided by AVISO as a by-product in order to compute Kinetic Energy (KE) and Eddy Kinetic Energy (EKE).

The Sea Surface Temperature (SST) data used in this work have been computed and made available by the GOS (Gruppo di Oceanografia da Satellite – ISAC CNR) (Marullo *et al.*, 2007). The product is GOS-L4HRfnd-MED_DTv1. All GOS products are based on the measurements obtained by available satellite infrared sensors (AATSR, AVHRR, MODIS, SEVIRI). Level 4 data provided by GOS-ISAC CNR represent the foundation SST (i.e. the temperature at the base of the daily thermocline) at midnight. SST data are available daily at a spatial resolution of $1/16^\circ$.

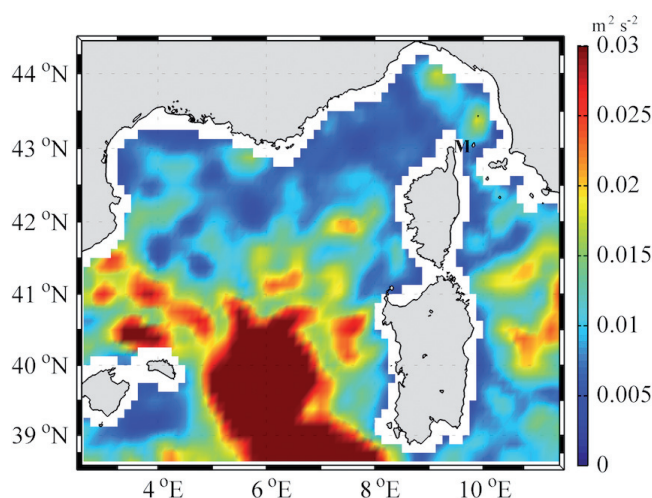


Fig. 1: Eddy kinetic energy computed from MSLA using AVISO data. The letter M indicates the approximate location of the underwater station.

Yearly Maps at 9 km resolution of sea surface chlorophyll concentration have been extracted by GIOVANNI (GES-DISC Interactive Online Visualization AND aNalysis Infrastructure) (Acker & Leptoukh, 2007). Chlorophyll data were derived from the MODIS-Moderate Resolution Imaging Spectroradiometer mounted on the Aqua platform.

In situ Data

Within the Corsica Channel there is an underwater station at about 450 m depth managed by CNR ISMAR (La Spezia). The station is located between the islands of Capraia and Corsica (labelled ‘M’ in Fig. 1), at the sill of the channel. It measures ocean currents and thermohaline properties of water masses at fixed depths continuously, for monitoring surface and intermediate circulation of the Mediterranean Sea, and exchanges between the two adjacent basins (Tyrrhenian Sea and Ligurian Sea). It has been active since 1985. The site is part of the CIESM Hydrochanges Programme (see <http://www.ciesm.org/marine/programs/hydrochanges.htm> and Schroeder *et al.*, 2012). Data from 2009 and 2010 have been used to compute the northward velocity through the channel. Until March 2010, hourly velocity data at 4 discrete depths are available: 80 m, 125 m, 320 m and 415 m. Since March 2010, an acoustic velocity profiler (ADCP, RDI WH Longrange) has been installed on the mooring. It measures velocity data with a 2-hour interval in 24 16-m bins, from the bottom to the sea surface, allowing for much more accurate transport estimation. Nevertheless, in order to maintain coherence with the 2009-2010 time series, only velocities at the 4 discrete depths have been extracted from the ADCP data and used for transport calculation.

The Liguro-Provençal Regional Ocean Modeling System

The Regional Ocean Modeling System (ROMS) (Shchepetkin & McWilliams, 2003, 2005) was configured for the North-western part of the Mediterranean Sea. ROMS solves the primitive equations based on the Boussinesq approximation and hydrostatic vertical momentum balance. In the NW Mediterranean model solutions for 2009 and 2010, the model domain extends from 37.8 N to 44.5 N and from 2 E to 16.5 E. The bottom topography is derived from the 30 arc-second resolution GEBCO database (www.gebco.net). In the adopted configuration, there are two open lateral boundaries: at 37.8 N and 2 E. We have chosen a horizontal resolution of 1/32°. At this resolution, the Rossby radius of deformation of the order of 5 – 12 km in the whole Mediterranean and for different seasons (see Grilli & Pinardi, 1998) is resolved. The model configuration is consequently adequate to simulate mesoscale and sub-mesoscale structures. The model grid has 35 vertical levels with vertical refinement near the sur-

face to obtain a satisfactory representation of the surface layer and the euphotic zone with a maximum of about 5 m (dz) of vertical discretisation in the euphotic zone. At the open lateral boundaries the model is forced with temperature, salinity and velocity fields obtained from the MERCATOR product PSY2V3 (www.mercator-ocean.fr). MERCATOR has a horizontal spatial resolution of 1/12° with daily outputs. At the sea surface, the regional ocean circulation model was forced with monthly mean climatology of heat and freshwater fluxes derived from the Comprehensive Ocean-Atmosphere Data Set (COADS; da Silva *et al.*, 1994). For the atmospheric momentum, wind-stress was extracted from the Limited Area Model Italy (COSMO-I7). COSMO-I7 (Montani *et al.*, 2003) is a non-hydrostatic and fully compressible numerical weather prediction model, which is a regional version of the Lokal Model (Doms & Schattler, 2002) regularly used for operational and research applications. The COSMO-I7, 3 hourly solutions, has a horizontal resolution of 1/16°. Validation of the COSMO-I7 wind fields has been widely performed (Steppeler *et al.*, 2003).

Eddy detection algorithm

In order to detect and track eddies from our numerical solution we adopted the “Vector Geometry-Based Eddy Detection Algorithm” (Nencioli *et al.*, 2010). The algorithm represents an alternative to other existing approaches such as Okubo-Weiss Parameter (Isern-Fontanet *et al.*, 2003; Chelton *et al.*, 2007), the wavelet analysis (Doglioli *et al.*, 2007) and the winding angle method (Sadarjoeen & Post, 2000; Chaigneau *et al.*, 2008). Preliminary results using the Okubo-Weiss method revealed that in the coastal zone of our study area strong frontal regions are often associated with values of Okubo-Weiss parameter (W) similar to eddy features. This made difficult the choice of threshold values capable of distinguishing between the two. The “Vector Geometry-Based Eddy Detection Algorithm” is a new method entirely based on geometrical characteristics of the flow field; it identifies eddies based on the shape or curvature of the instantaneous streamlines. The method is particularly appropriate for the analysis of eddy activity from the results of high-resolution numerical experiments (Nencioli *et al.*, 2010). With this method, four parameters have to be defined: (i) the first parameter, (a), defines how many grid points in magnitude of v (along the E–W axes) and u (along the N–S axes) are checked; (ii) the second parameter, (b), defines the dimension, in terms of grid points of the area used to define the local minimum of velocity; (iii) the third parameter, (r), is the number of grid points required to define the initial area and compute eddy dimensions; (iv) the fourth parameter, (rad), is the searching area used to track the centre of the eddies at successive time steps. A good estimate for the searching area dimensions, since eddies are advected by the local currents, can be derived by multiplying the average current speed by the

dataset sampling period as mentioned in Nencioli *et al.* (2010). A complete description of parameters and the eddy detector and tracking algorithm is included in Nencioli *et al.* (2010). After a few sensitivity tests for the region of interest, a set of parameters was tuned ($a=4$; $b=3$; $rad=8$; $r=14$), and only eddies with a lifetime greater than 5 days, were considered.

Data Analysis

The analyses performed in this work investigate the oceanographic processes linked to the productivity of the North-Western Mediterranean Sea at three different spatial and temporal scales.

Large scale processes have been investigated in the area extending from 38.8° N to 44.5° N and from 2.5° E to 11.5° E. At large scale, we used yearly average maps of sea surface chlorophyll concentration to detect and map the productive zone of the study area. To investigate ecosystem dynamics we focus the attention on the inter-annual variability in the spatial distribution of patches of high chlorophyll concentration. We used oceanographic model solutions to map yearly averaged streamlines as a mirror of the main circulation path of the study area. We then performed an eddy census for year 2009 and year 2010. The aim of this large scale analysis is to depict the large scale scenario of the main processes of the area, to show the spatial distribution of the main chlorophyll patch and to focus attention, even at large scale, on the processes investigated in this work: distribution of eddies and their role. The analysis of eddies and their impact on the distribution of properties is then carried at local scale.

At the regional scale, the area has been divided into three boxes (labelled b1, b2, b3 in Fig. 3), which extend respectively from 42.9° N to 44.5° N and from 6.2° E to 11.5° E; from 41° N to 42.9° N and from 5° E to 8° E; from 41° N to 42.9° N and from 8° E to 11.5° E. In particular, we used the three boxes for ROMS_NWMed data comparison (see paragraph 2.6), while for the main purpose of this paper, we used only box b1 as it covers the area where the greater variability of the bloom occurs. We then looked at differences in sea surface chlorophyll concentration during the two years analysed. We also looked at mean KE and EKE in the same period (computed from AVISO MADT and MSLA respectively). Finally, we analysed eddies distribution, lifetime and nature during the period from January to April of both years. The processes occurring during these months are those most affecting the bloom, as they determine the spring vertical stratification and other conditions (e.g. distribution of nutrients) that trigger the spring chlorophyll bloom.

We conclude our analyses by looking directly at mesoscale processes. We focus on specific eddies, describing their location, kinetic energy and their impact on the MLD and on vertical mixing.

The MLD is set by the balance of processes that

tend to stabilise and destabilise the density structure of the upper ocean and it is of crucial importance for the modulation of biochemical cycles (Troupin *et al.*, 2010), which are directly affected by the variations of the physical variables in the euphotic zone. We use then the depth of the MLD as a proxy of ecosystem production, as environmental forcing controls spatio-temporal changes in phytoplankton abundance and community composition by affecting the key determinants of marine photosynthesis such as mixed-layer light availability, concentration of macronutrients and micronutrients, and the ambient temperature (Field *et al.*, 1998; Behrenfeld *et al.*, 2002).

Eddies are the local process, investigated in this work, which act to destabilise the density structure of the surface layers at local scale due to the complex pattern of intense vertical velocity associated with the eddy structure (Koszalka *et al.*, 2009; Casella *et al.*, 2011) and the action of recall water from the nearby surface or deeper layers. Consequently, eddies have an impact on the variation of the MLD (Khöl, 2007).

The MLD, in this work, is defined within the ROMS K-Profile Parameterization (KPP, Large *et al.*, 1994). The MLD is defined as the depth d at which the bulk Richardson number, which measures the ratio between stratification and shearing, is equal to a prescribed critical value:

$$Ri_b(d) = \frac{[B_r - B(d)]d}{|V_r - V(d)|^2 + V_t^2(d)} = Ri_{cr} = 0.3$$

Where B_r and V_r are estimates of the average buoyancy and velocity, respectively, and V_t is the turbulent velocity shear.

Moreover, we used the vertical mixing coefficient to indicate vertical displacement and changes in the vertical structure of the ocean, and consequently the distribution of environmental variables affecting productivity. In this work, we extracted the vertical mixing coefficient corresponding to selected eddies in order to measure the influence of eddies on vertical mixing. The area dominated by the presence of an eddy is computed by the eddy detection algorithm (Nencioli *et al.*, 2010) and the vertical mixing coefficient at 20 m depth has been extracted in correspondence with the eddy area. In this work, the vertical mixing coefficients for tracers is computed with the Large *et al.* (1994) mixing scheme.

Results

ROMS_NWMed data comparison

The model results have been assessed against the available data, both in situ and remote sensed.

First, in order to evaluate the ability of the model in simulating currents along the water column, we have compared the two years (2009, 2010) of ROMS_NWMed numerical simulations with data collected by the current-

meters deployed in the Corsica Channel. The modelled equivalent mean current is in good agreement with the measured data, for the same approximate location. The current has the same general direction (north), and comparable magnitudes ($0.3\text{--}0.5\text{ ms}^{-1}$ in winter; $0.1\text{--}0.2\text{ ms}^{-1}$ in summer), as well as the same seasonal variability (Fig. 2). Figure 2 shows the comparison between the meridional velocity measured by the currentmeter nearest to the surface, which is located at about 80 m depth, and the meridional velocity computed by the model at the same approximate location. The same simulation was previously validated (Caldeira *et al.*, 2012) by comparing the Corsica Channel transport with mooring observations showing that the simulated transport has a general trend similar to the measured one and a comparable magnitude and seasonal variability with a Mean Absolute Difference (MAD), for the two-year time series, of 0.44 Sv . The general good agreement of the variability of the simulated current entering in the domain with the measurements discussed in this section, is at the base of our study since eddies, which are the main local process under investigation in this work, generate from the instability of the Northern Current, which originates in part from the ECC.

Secondly, maps of simulated surface KE computed from the model's geostrophic velocities (derived from surface elevation) have been interpolated on a $1/8^\circ$ resolution grid in order to be compared with maps of KE from AVISO maps. The MAD has been computed using the formulation

$$\left\langle \sqrt{\left((X - X_0)^2 \right)} \right\rangle$$

where $\langle \rangle$ represents the temporal mean, X represents the modelled KE and X_0 the KE from AVISO data. The spatial MAD from AVISO and ROMS_NWMed data is shown in Figure 3 for the simulated period. Figure 3 shows that the highest values of MAD are located in coastal areas corresponding to high dynamic zones such

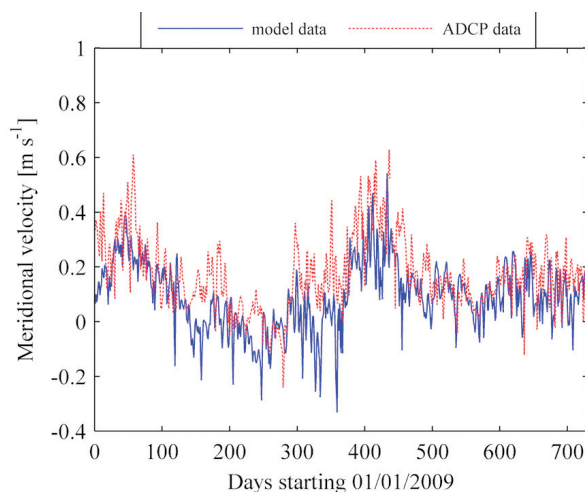


Fig. 2: Time series of surface meridional velocity in the Corsica Channel for the period 2009 - 2010. Red dashed line: meridional velocity from current meters and ADCP data. Blue continuous line: meridional velocity from ROMS_NWMed data.

as the Liguro-Provençal current. The northern part of the basin has been divided into three main boxes (b1, b2, b3 in Figure 3) with different hydrodynamic characteristics. Figure 4 shows the time series of spatial averaged KE for each box computed from the AVISO data set and ROMS_NWMed model. Boxes b1 and b3 include the coastal zone while b2 is an open ocean zone. The time series (Fig. 4) shows that there is a significant difference between AVISO and ROMS_NWMed KE in box b1 and b3 while the MAD in box b2 is the lowest with a mean value of $7.1 \cdot 10^{-3}\text{ m}^2\text{ s}^{-2}$. In the area known as a low dynamic zone (box b2) the agreement between AVISO and ROMS_NWMed KE is higher. The areas dominated by high dynamics (boxes b1 and b3) have a higher discrepancy between AVISO and ROMS_NWMed KE. In these regions, the altimetry has some critical limiting factors because of the ageostrophic dynamics induced by lateral and bottom boundaries and nearshore forcings (Csanady, 1982), such as the presence of land mass and inaccuracies of geophysical corrections (Bouffard *et al.*, 2008). Moreover, for the purpose of this work, the main limit of the altimetry data, in these areas, is due to the resolution of the product. These areas are characterised by the development of a significant number of mesoscale eddies with a diameter between 15-20 km (tab. 2) (see also Casella *et al.*, 2011; Hu *et al.*, 2011; Kersalé *et al.*, 2013). Since the spatial resolution of the altimetry is about 14 km, this product has some limits in catching these mesoscale structures and the dynamics induced by them. Due to these factors, boxes b1 and b3 show a significant difference between the time series of averaged KE from AVISO and ROMS_NWMed data while in box b2, defined as a calm area characterized by an insignificant presence of small-scale structures, the differences between AVISO and ROMS_NWMed data is nearly null.

Finally, we compared the SST product of CNR-GOS and ROMS_NWMed SST (Fig. 5). Even though the model

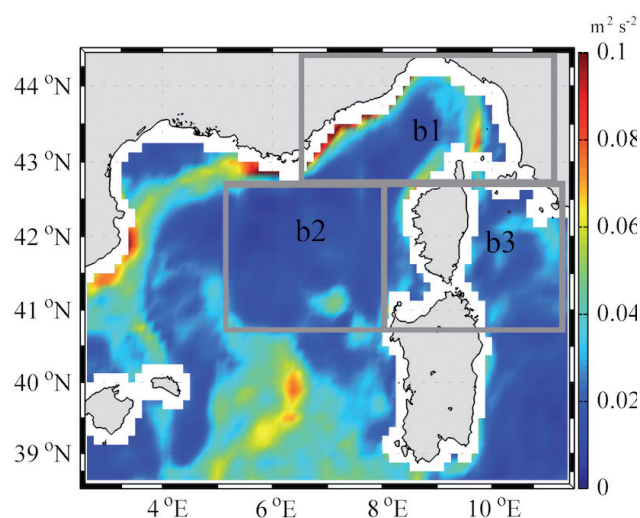


Fig. 3: Mean Absolute Difference of Kinetic Energy based on AVISO and ROMS_NWMed data.

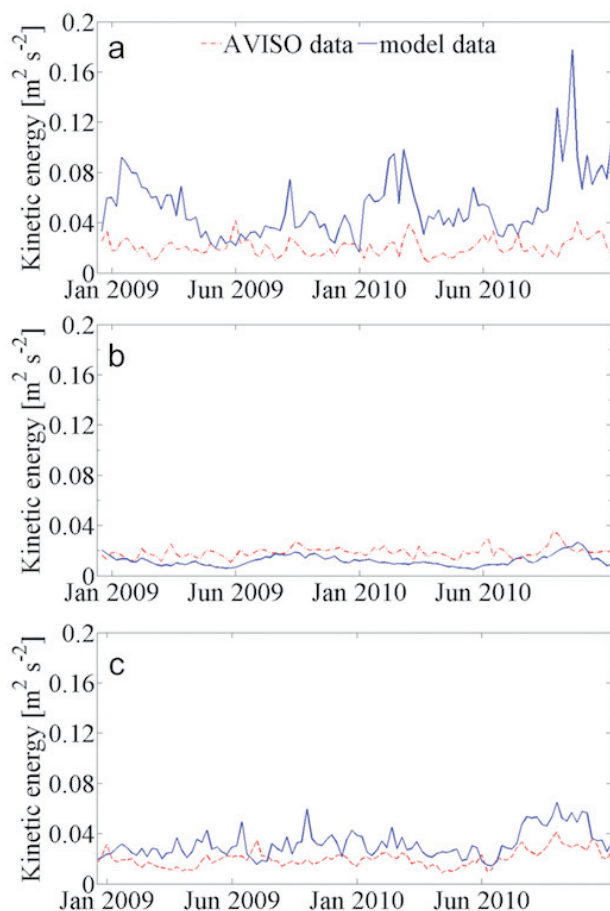


Fig. 4: Kinetic Energy in boxes b1 (panel A), b2 (panel B), b3 (panel C) indicated in figure 3. Time series 2009 - 2010. Red dashed line: AVISO KE product. Blue continuous line: ROMS_NWMed KE.

at the surface boundary is forced by the monthly mean climatologies of heat derived from COADS data set, the averaged SST time series, for the two years simulated, shows that the model is able to reproduce both seasonal and inter-annual SST fluctuations (Fig. 5) with a MAD of 0.87 °C.

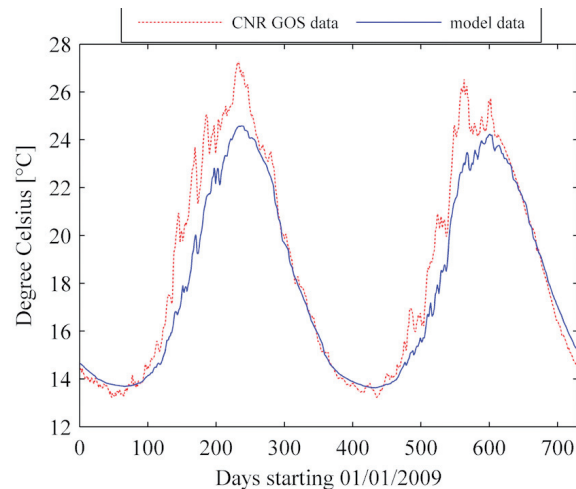


Fig. 5: SST time series 2009 2010. Red dashed line: CNR-GOS SST product. Blue continuous line: ROMS_NWMed SST.

The paper by Caldeira *et al.* (2012) shows good agreement of the spatial distribution of the SST variable between simulated and satellite derived data.

Large scale analysis

The analysis of yearly mean ocean colour data confirms the persistent existence of a productive zone in the central part of the Liguro-Provençal basin during 2009 and 2010. Figures 6A and B show the spatial distribution of yearly-averaged sea surface chlorophyll concentrations in 2009 and 2010, together with model streamlines. We verified, after analysing the distribution of chlorophyll during the blooming period, that the main patch of the yearly-averaged chlorophyll concentration maintains the imprint of the spatial distribution occurring during the spring bloom. Streamlines in Figures 6A and B show a dynamic region in correspondence of the rim. This area is dominated by the ECC, the WCC and the Northern Current. As a consequence, this area is characterized by low chlorophyll concentration. The central area, where streamlines clearly indicate the presence

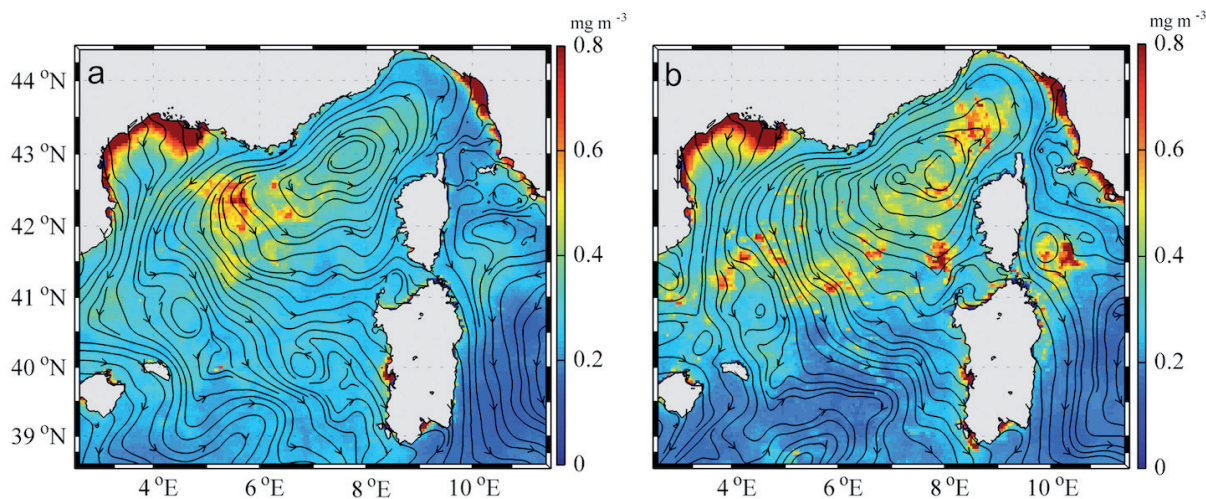


Fig. 6: Yearly averaged chlorophyll concentration based on MODIS data with yearly averaged ROMS_NWMed model streamlines in 2009 (panel a) and 2010 (panel b).

of a large cyclonic gyre, shows a high chlorophyll concentration. We highlight the inter-annual variability in the location of the main chlorophyll patch. The patch of higher chlorophyll concentration is not located in the same location inside the cyclonic gyre in the two years. In fact, in 2009 the main bloom occurred in the South-western part of the basin, as suggested by a higher chlorophyll concentration patch located approximately 100 km offshore of Marseille (France). In 2010, the main patch is located in the North-eastern part of the basin. These differences have been ascribed to locally enhanced variability, which reflects the role of coastal interactions, local processes and atmospheric forcing in the fertilization process (Barale *et al.*, 2008). As a matter of fact, the general circulation process of the area, simulated by ROMS_NWMed and described by yearly averaged streamlines, shows a similar scenario in both years. Streamlines in Figures 6A and B depict the main path of the cyclonic gyre, which represents the well-known circulation (Alberola *et al.*, 1995; Conan & Millot, 1995; Sammari *et al.*, 1995; Millot, 1999; Robinson *et al.*, 2001; André *et al.*, 2005). Together with the cyclonic circulation, which broadly surrounds the productive area, the model solutions also show intense eddy activity in the rim. Eddies are located along the path of ECC, WCC, and Northern Currents and, in general, along dynamic areas (Fig. 7). The analysis of the concurrent AVISO altimetry data for 2009 and 2010 confirms that the region surrounding the Liguro-Provençal Basin has the most intense KE values (Fig. 7). Figure 7 also shows the track of eddies detected in the simulation for year 2009. Both cyclonic (black colour) and anticyclonic (grey colour) eddies are generally located in the most dynamic areas. In the central part of the basin no eddies are detected.

Regional scale analysis

At the regional scale, the Northern part of the basin (box b1 indicated in Fig. 3) shows high chlorophyll inter-annual variability. In fact, in box b1, the averaged chlorophyll concentration during the 2009 bloom period is 0.7 mg.m^{-3} while during the 2010 bloom period its value reaches 1.0 mg.m^{-3} (Table 1). This interannual variability, as discussed in the introduction, is due to local and regional hydrodynamic processes (Barale *et al.*, 2008). Here, we investigate the local processes associated to the distribution, tracks, lifetime and nature of eddies during the period from January to April for the years 2009 and 2010.

Table 1 summarises the chlorophyll concentration, eddies number, type and lifetime. Figures 8A and b show the tracks of eddies superimposed on AVISO KE for the years

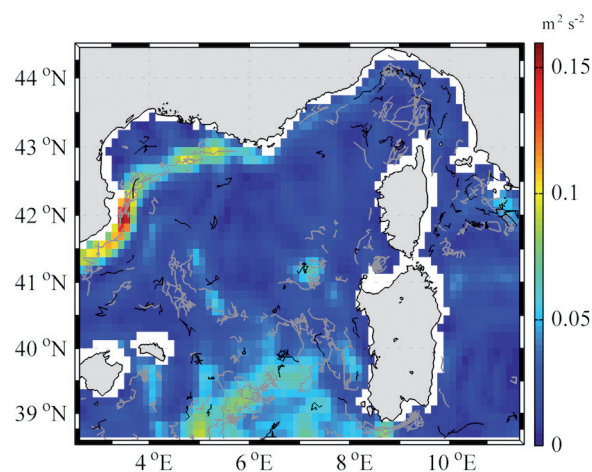


Fig. 7: Yearly averaged Kinetic Energy based on AVISO data with ROMS_NWMed model eddy tracks in 2009. Black colour indicates cyclonic eddy track; Grey colour indicates anticyclonic eddy track.

2009 (Fig. 8A) and 2010 (Fig. 8B). Eddies are present in both periods and are located near areas with high AVISO KE value, which indicate the presence of the Northern Current. During Jan-Apr 2009, 6 eddies were detected in the realistic ROMS_NWMed solutions in box b1, 50% were cyclonic;

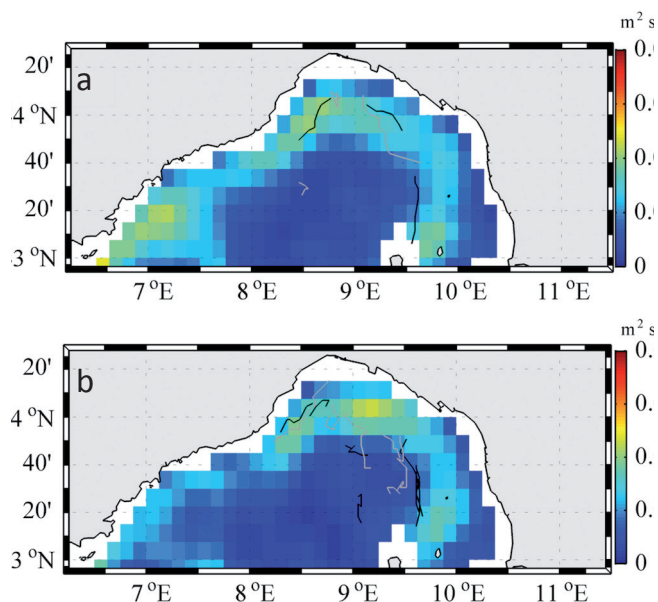


Fig. 8: Averaged Kinetic Energy during Jan-Apr from AVISO superimposed with eddies tracks from ROMS_NWMed model for the years 2009 (panel a), 2010 (panel b). Black colour indicates cyclonic eddy track; Grey colour indicates anticyclonic eddy track.

Table 1. Differences in terms of chlorophyll concentration, eddies number, type, maximum lifetime and total lifetime (sum of eddies lifetime) during the period from January to April for the years 2009 and 2010.

| Year | Avg Chla [mg m ⁻³] | Eddies number | | | Max lifetime [d] | Tot. lifetime [d] |
|------|-----------------------------------|---------------|----------|--------------|---------------------|----------------------|
| | | Tot [nb] | Cyclonic | Anticyclonic | | |
| 2009 | 0.7 | 6 | 50% | 50% | 9 | 43 |
| 2010 | 1.0 | 13 | 60% | 40% | 18 | 114 |

whereas during the Jan-Apr 2010 simulation, 13 eddies were counted, 8 (60%) cyclonic and 5 (40%) anticyclonic. The lifetime of anticyclonic eddies is higher in both years. In 2009, the maximum value of lifetime is 9 days while in 2010 it reaches 18 days. Finally, the total time of eddy occurrence (i.e. the sum of eddies lifetime in days) is 43 for 2009 and 114 for 2010.

For 2010, the analysis reported a higher number of eddies with a longer lifetime. This higher eddy activity in the area during 2010 is also confirmed by AVISO EKE for the same period of time. Figures 9A and B show the tracks of eddies superimposed on AVISO EKE during the period Jan-Apr for the years 2009 (Fig. 9A) and 2010 (Fig. 9B). In spite of the AVISO limits in catching (sub) mesoscale processes in the small area investigated (due to its resolution), the figures show higher values of EKE. This is a measure of the intensity of mesoscale activity, and suggests that intense eddy activity occurs in the area.

Mesoscale processes analysis

The simulated eddies can be divided in two main categories, on the basis of their location:

1. eddies located between the coastline and the current.

Figure 10 shows two structures: a cyclonic eddy (A) and an anticyclonic eddy (B) trapped between the coastline and the Northern Current. The colour depicts the MLD and the vectors indicate the current direction at 50 m depth. The two vortices interact with each other and they both interact with the Northern Current, which is detached from the coastline by the action of the two vortices. The MLD is highly affected by the presence of the two eddies. In particular, the anticyclonic eddy has a stronger effect on the MLD in the central part of the

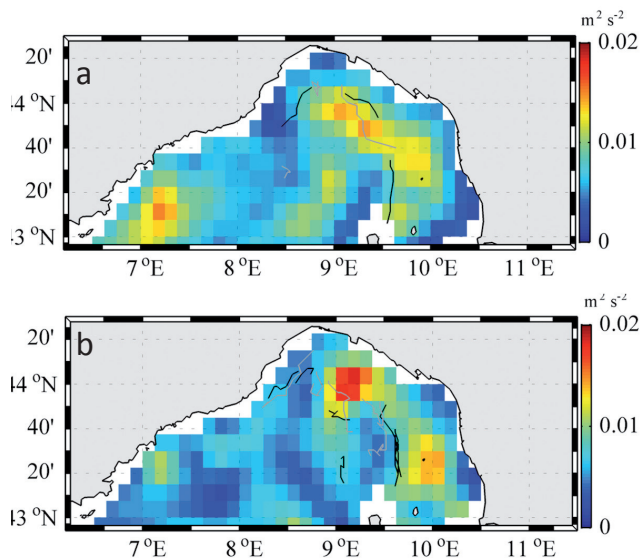


Fig. 9: Averaged Eddy Kinetic Energy during Jan-Apr from AVISO superimposed with eddies tracks from ROMS_NWMed model for the years 2009 (panel a), 2010 (panel b). Black colour indicates cyclonic eddy track; Grey colour indicates anticyclonic eddy track.

structure while the cyclonic eddy has a marginal impact in correspondence with its boundaries. The MLD corresponding to the anticyclonic eddy reaches the value of 160 m, while the value of the surrounding environment is in the order of 30-50 m.

2. eddies located between the current and the central basin.

This type of eddy is illustrated in Figure 11A. The figure shows an anticyclonic eddy (A) and the last day of life of a cyclonic eddy (B) squeezed between the Northern Current and the anticyclonic eddy. The tracks of the two eddies are located north of Corsica, between the current and the central part of the basin. They both interact with the Northern Current. The MLD in the central part of the anticyclonic eddy reaches 80 m showing the effect of the eddy on the mixing layer. Figure 11B shows the KE corresponding to the anticyclonic eddy at 50 m depth. The maximum values of KE are located at the vortex edges (Fig. 11B). From the surface down to 50 m depth, the values of KE corresponding to the vortex have the same order of magnitude as the values generated by the Northern Current.

Both types of eddy can act as localised pumps of nutrients due to their high total time of eddy occurrence (43 for Jan-Apr 2009 and 114 for Jan-Apr 2010); the second type, located between the Northern Current and the central basin, can increase the concentration of nutrients directly in the chlorophyll bloom area. The location and tracks of eddies shown in Figure 8 indicate a predominance of second type eddy for the year 2010.

For the year 2010, a deeper analysis has been undertaken to unravel the influence of the detected eddies on vertical mixing. As previously indicated in Table 1, 13 eddies, with a lifetime greater than 5 days, have been detected from January to April 2010 in the Northern part of the basin (box b1, Fig. 3). The tracks of the 13 eddies are shown in Figure 8B. Hereafter, we quantify the properties of these 13 eddies and their impact on the area dominated by their presence.

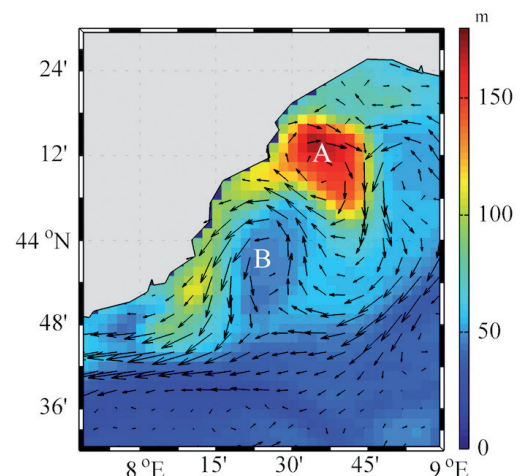


Fig. 10: Mixed Layer Depth and speed vectors at 50 m depth from the ROMS_NWMed model on 28 March 2010.

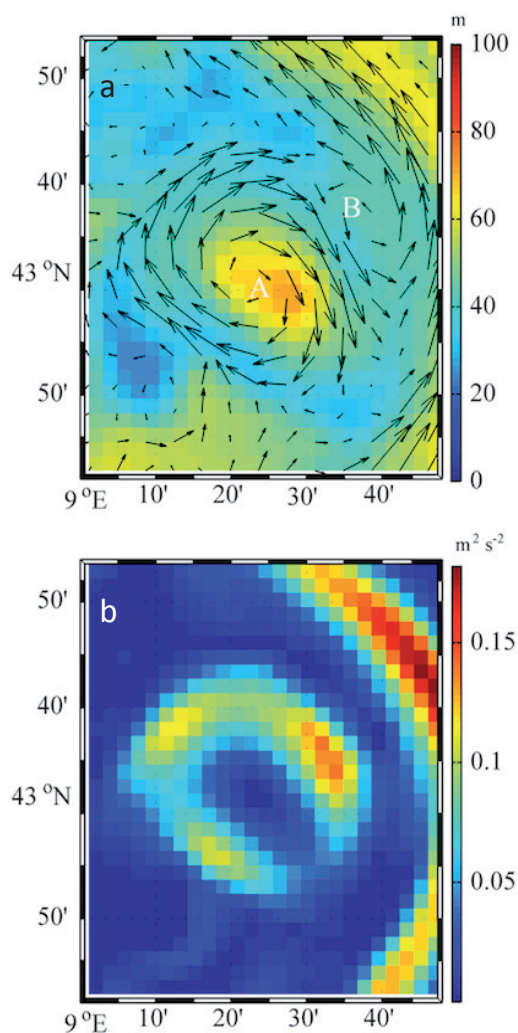


Fig. 11: Mixed Layer Depth, speed vectors (panel a) and Kinetic Energy (panel b) at 50 m depth from ROMS_NWMed model on 25 March 2010.

For each of the 13 eddies detected, Table 2 shows their nature (cyclonic/anticyclonic), lifetime, birth day, averaged daily diameter, averaged daily area, number of days in which the eddy strongly affects the MLD and averaged vertical mixing coefficient for tracers (AKt). We estimated that the eddy affects the MLD when the difference between the MLD in the area dominated by the eddy and in the surrounding area is greater than 10 m. From this assumption, we derived the number of days in which the eddy strongly affects the MLD.

From this analysis, we can compute the total area of MLD affected by the presence of the eddies in the first 4 months of the year by multiplying the sum of the number of days in which the eddy strongly affects the MLD and the sum of the averaged daily area. The total area of MLD affected by the presence of the eddies is around 360,000 km², which is almost seven times the entire study area (box b1, Figure 3).

The vertical mixing coefficient has been extracted in correspondence with the area dominated by the eddy at 20 m depth and averaged on the eddy lifetime. We chose the depth of 20 m since all 13 eddies investigated reach and affect more than the first 20 m of water column. The value of the averaged vertical mixing coefficient is higher for eddies that develop during the winter period here investigated (Jan-Feb); this is due to the winter weak stratification. Moreover, during this period, both cyclonic and anticyclonic eddies affect the vertical mixing with values reaching 0.1 m²s⁻¹. During spring, the averaged value of the vertical mixing coefficient corresponding to eddies decreases, although for specific days we still observe values of the vertical mixing coefficient reaching 0.1 m²s⁻¹ in correspondence with an eddy. As an example, Figure 12 shows the spatial distribution of the vertical mixing coefficient for tracers, at 20 m depth, and

Table 2. Nature (cyclonic/anticyclonic), lifetime, birth day, averaged daily diameter, averaged daily area, number of days in which the eddy strongly affects the MLD and averaged vertical mixing coefficient for tracers (AKt) for eddies detected during the period from January to April for the year 2010.

| Eddy | C/A | Lifetime | Birth Day | Avg daily Diameter [km] | Avg daily Area [km ²] | Nb of days affecting MLD | Avg Akt [m ² s ⁻¹] |
|------------------|-----|------------|-----------|-------------------------|-----------------------------------|--------------------------|---|
| 1 | C | 8 | 8 Jan | 20 | 309 | 6 | 0.1398 |
| 2 | C | 8 | 17 Feb | 23 | 400 | 4 | 0.0972 |
| 3 | A | 8 | 19 Feb | 23 | 398 | 8 | 0.1693 |
| 4 | A | 12 | 28 Feb | 23 | 416 | 10 | 0.1032 |
| 5 | C | 6 | 12 Mar | 15 | 172 | 5 | 0.0437 |
| 6 | C | 7 | 19 Mar | 16 | 191 | 3 | 0.0272 |
| 7 | C | 7 | 25 Mar | 13 | 126 | 4 | 0.0459 |
| 8 | A | 11 | 26 Mar | 23 | 409 | 9 | 0.0531 |
| 9 | A | 18 | 21 Mar | 27 | 588 | 16 | 0.0344 |
| 10 | A | 9 | 10 Apr | 22 | 373 | 7 | 0.0046 |
| 11 | C | 8 | 13 Apr | 11 | 96 | 3 | 0.0044 |
| 12 | C | 6 | 29 Apr | 17 | 223 | 4 | 0.0028 |
| 13 | C | 6 | 29 Apr | 30 | 689 | 4 | 0.0042 |
| Tot (sum) | | 114 | | | 4389 | 83 | |

the area dominated by the presence of the eighth eddy on the 1st of April (white contour line). The value of the vertical mixing coefficient corresponding to the eddy is higher than the surrounding area and it is of the same order of magnitude as regards other processes affecting the region.

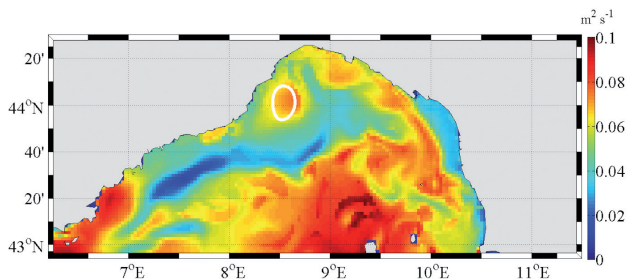


Fig. 12: Spatial distribution of vertical mixing coefficient for tracers, at 20 m depth, and area of the eighth eddy on the 1st April 2010 (white contour line).

Discussion

In this study, a multi-scale approach has been used for the investigation of the chlorophyll bloom and its variability in the location of the main patch in the North-western Mediterranean Sea. As evidenced by MODIS Chlorophyll data, the Liguro-Provençal Basin is affected by significant interannual variability in chlorophyll concentration and distribution. At large scale, it is evident how the main patch of chlorophyll lies in the North-western basin, within the well known cyclonic gyre but it is not located in the same place in the two years investigated. Comparing Chlorophyll maps from 2009 and 2010, we notice a significant displacement of this patch. This displacement is due to local and regional hydrodynamic factors. The analysis of concurrent AVISO altimetry data evidences that the region surrounding the Liguro-Provençal Basin has the most significant KE values. While high values of KE and EKE are usually associated with productive regions, here we find an opposite situation. In fact, the most productive regions correspond to lower KE and EKE values, when compared to the entire study area. The fact that the highest KE and EKE values are found along the borders of the productive area, and in particular along the Northern Current, suggests that we need to investigate processes at a different scale. The simulation of the Northern Current in the Ligurian Sea with a high-resolution, primitive equation model (ROMS), reveals the formation of mesoscale eddies along the current. Our simulation is in good agreement with the findings of Sammari *et al.* (1995), who observed eddy formation along this current.

In this work, we investigated the daily presence and distribution of these eddies. The depicted scenario for the whole year shows that eddy tracks are mainly located along the dynamic boundary current. In order to inves-

tigate the possible role of these eddies in affecting the spring bloom, we concentrated our study on their interannual variability. We considered only those months where the processes most affecting the spring bloom occur, and consequently we analysed eddies from January to April for each year. The main process driving the spring bloom in the Ligurian Sea is the intense winter vertical convection, which mixes the cool dense surface water and the underlying saltier and nutrient-rich water masses. The spring bloom does not occur homogeneously within the study area. As a matter of fact, in the Northern part of the basin (box b1), a strong chlorophyll bloom occurs during 2010, while 2009 appears as a low-chlorophyll concentration year. We analysed the distribution of vortices and their impact on the MLD and on the vertical mixing and we found that they interact with the Northern Current and with each other, acting as localized long-lived nutrient pumps. The Northern Current can then be described as a highly dynamic rim of eddies. This rim and its associated eddies have the potential to allow the transport of nutrients both from the eddy-induced vertical mixing and the nearby coastal regions. The central and less turbulent zone, on the other hand, can be described as a pool, where nutrients trigger the main spring bloom. The pool represents the central zone characterised by a stable surface layer rich in nutrients where phytoplankton can develop and the pool is bordered by a highly dynamic ring where phytoplankton lacks the factors necessary for its development.

As shown by the ROMS_NWMed simulation, eddies in the rim are characterized by a long lifetime and closed streamlines. Eddies are then associated with a dominance of rotation over strain. The strong vertical velocities, shown in correspondence with the eddies simulated in the Ligurian Sea by Casella *et al.* (2011), are associated with these vortices and they can induce exchanges between the surface layers and the nutrient-rich deeper layers. Among the two years considered here, a significantly higher number of eddies is found during the chlorophyll-rich 2010. Moreover, during this year eddies showed a longer lifetime with a total time of eddy occurrence during Jan-Feb of 114 days. On the contrary, in 2009, when a poorer bloom occurred in the region, a lower number of eddies with a shorter lifetime are found, with a total time of eddy occurrence during Jan-Feb of 43 days. The interannual variability of eddy distribution during the period affecting the spring bloom in the Northern part of the basin (box b1, Fig. 3) can be correlated with the chlorophyll concentration. The year 2010 is a chlorophyll-rich year and it has a higher number of eddies, which act as a localised pump of nutrients due to their action on MLD and vertical mixing; therefore, the action of eddies can be considered as one of the local processes affecting the location of the main chlorophyll patch.

In order to investigate how eddy dynamics influence ecosystem production in more detail, we looked at the

displacement of the MLD and the values of the vertical mixing coefficient for tracers corresponding to eddies. The analysis of the spatial scale of these processes reveals that eddies significantly affect the MLD, and the temporal scale analysis shows that eddies affect the MLD for several days during their lifetime. Both cyclonic and anticyclonic eddies affect the MLD. In particular, the anticyclonic eddies deepen the MLD stronger than the cyclonic eddies and consequently they both influence the process of water exchange between surface and deeper layers, where nutrients lie, thus affecting the fertilization process (Fig. 9 and 10A). Furthermore, high KE values have been found in correspondence with eddy edges (Fig. 10B), highlighting the importance of the dynamics of these structures. The role of eddies in the fertilization process seems to be confirmed by their higher number, type and longer presence from January to April 2010 when compared to the previous year. The total area of MLD affected by the presence of the eddies, from January to April 2010, with a lifetime greater than 5 days, is around 360,000 km². This underlines the dimension of this localised process during 4 months.

The extraction of the vertical mixing coefficient for tracers in correspondence with eddies has been used to estimate the impact of eddy presence on ecosystem production. Both cyclonic and anticyclonic eddies affect the vertical mixing coefficient. In general, the analysis undertaken allows to underline the importance of eddies as a localised process, affecting the vertical displacement of properties. In turn, this localised process is affected by the main dynamics and by the seasonality of the basin. In fact, the analysis of the vertical mixing coefficient reveals the effect of eddies on the vertical displacement but, in general, the intensity of this coefficient in the whole basin is modulated by seasonal stratification.

In conclusion, the results reported in this work indicate the importance of mesoscale structures in the Ligo-ro-Provençal Basin and their possible contribution to the location of the main fertilization process.

Acknowledgements

We thank the two anonymous reviewers for their useful criticism and suggestions, which helped to improve this paper significantly. Two of the authors, EC and PT, are grateful to the CIMA Research Foundation for support and travel funds, which enabled researchers to concretise this collaboration, and to CCM for hosting the researchers in Madeira. Numerical model solutions were calculated at CIIMAR HPC unit, constructed using funds from the FCT Portuguese National Science Foundation and from RAIA (0313 RAIA 1 E) and the RAIA.co projects, co-funded by INTERREGIV and FEDER ('Fundo Europeu de Desenvolvimento Regional, 20072013'), through the POCTEP regional initiative. We thank Anne

Molcard (Univ. Toulon) and Anna Vetrano (CNR-IS-MAR) for useful discussions. We are also indebted to the technical staff of ISMAR, and particularly to Mireno Borghini, for assistance in the collection and processing of mooring data. The altimeter products were produced by SSALTO/DUACS and distributed by AVISO with support from CNES. MODIS-Aqua data was extracted using the Giovanni on line data system, developed and maintained by the NASA GES DISC. One of the authors, EC, is grateful to the MIRAMar project sponsored by PO CRO European Social Fund, Regione Liguria 2007-2013 Asse IV "Capitale Umano / Human Capital" for support.

References

- Acker, J.G., Leptoukh, G., 2007. Online analysis enhances use of NASA Earth science data. *EOS, Transactions American Geophysical Union*, 88 (2), 14-17.
- Abraham, E., 1998. The generation of plankton patchiness by turbulent stirring. *Nature*, 391, 577-580.
- Alb  rola, C., Millot, C., Font, J., 1995. On the seasonal and mesoscale variabilities of the Northern Current during the PRIMO-0 experiment in the western Mediterranean Sea. *Oceanologica Acta*, 18 (2), 163-192.
- Andr  , G., Garreau, P., Garnier, V., Frauni  , P., 2005. Modelled variability of the sea surface circulation in the North western Mediterranean Sea in the Gulf of Lions. *Ocean Dynamics*, 55, 294-308.
- Arnone, R., 1994. The temporal and spatial variability of chlorophyll in the western Mediterranean, in Seasonal and Interannual Variability of the Western Mediterranean Sea. *Coastal and Estuarine Studies, AGU, Washington, D.C.*, 46, 192-225.
- Barale, V., Jaquet, J.M., Ndiaye, M., 2008. Algal blooming patterns and anomalies in the Mediterranean Sea as derived from the SeaWiFS data set (1998-2003). *Remote Sensing of Environment*, 12, 3300-3313.
- Behrenfeld, M.J., Esaias, W.E., Turpie, K.R., 2002. Assessment of primary production at the global scale. p. 156-186. In: *Phytoplankton Productivity: Carbon Assimilation in Marine and Freshwater Ecosystems*. Williams P.J. le B. (Ed.). Blackwell Science, Oxford, U.K.
- Birol, F., M., Cancet, M., Estournel C., 2010. Aspects of the seasonal variability of the Northern Current (NW Mediterranean Sea) observed by altimetry. *Journal of Marine Systems*, 81, 297-311.
- Bouffard, J., Vignudelli, S., Cipollini, P., Menard, Y., 2008. Exploiting the potential of an improved multimission altimetric data set over the coastal ocean. *Geophysical Research Letters*, 35, L10601. doi:10.1029/2008GL033488.
- Bracco, A., LaCasce, J., Provenzale, A., 2000. Velocity probability density functions for oceanic floats. *Journal of Physical Oceanography*, 30, 461.
- Bracco, A., Chassignet, E.P., Garraffo, Z.D., Provenzale, A., 2003. Lagrangian velocity distribution in a high-resolution numerical simulation of the North Atlantic. *Journal of Atmospheric and Oceanic Technology*, 20, 1212-1220.
- Caldeira, R.M.A., Couvelard, X., Casella, E., Vetrano, A., 2012. Asymmetric eddy populations in adjacent basins – a high resolution numerical study of the Tyrrhenian and Ligurian Seas. *Ocean Science Discussion*, 9, 3521-3566.

- Casella, E., Molcard, A., Provenzale A., 2011. Mesoscale vortices in the Ligurian Sea and their effect on coastal upwelling processes. *Journal of Marine Systems*, 88, 12-19.
- Chaigneau, A., Gizolme, A., Grados, C., 2008. Mesoscale eddies off Peru in altimeter records: identification algorithms and eddy spatio-temporal patterns. *Progress in Oceanography*, 79, 2-4, 106-119.
- Chelton, D.B., Schlax, M.G., Samelson, R.M., de Szoeke, R.A., 2007. Global observations of large oceanic eddies. *Geophysical Research Letters*, 34, L15606. doi:10.1029/2007GL030812.
- Conan, P., Millot, C., 1995. Variability of the Northern Current off Marseilles, western Mediterranean Sea, from February to June 1992. *Oceanologica Acta*, 18 (2), 193-205.
- Csanady, G.T., 1982. *Circulation in the Coastal Ocean*. D. Reidel Publishing Co., Dordrecht, The Netherlands. 264 pp.
- da Silva, A.M., Young, C.C., Levitus, S., 1994. *Atlas of Surface Marine Data 1994. Volume 1: Algorithms and Procedures*. Technical Report NOAA Atlas NESDIS 6. National Oceanic and Atmospheric Administration, Washington, DC, 83 pp.
- Doglioli, A.M., Blanke, B., Speich, S., Lapeyre, G., 2007. Tracking coherent structures in a regional ocean model with wavelet analysis: application to Cape Basin eddies. *Journal of Geophysical Research*, 112, C05043. doi:10.1029/2006JC003952.
- Doms, G., Schattler, U., 2002. *A Description of the Nonhydrostatic Regional Model LM, Part I: Dynamics and Numerics*. LM F90 2.18, Deutscher Wetterdienst, Offenbach, Germany, 149 pp.
- D'Ortenzio, F., d'Alcalà, M.R., 2009. On the trophic regimes of the Mediterranean Sea: a satellite analysis. *Biogeosciences*, 6, 139-148.
- Ducet, N., Le Traon, P.Y., Reverdin, G., 2000. Global high resolution mapping of ocean circulation from the combination of TOPEX/POSEIDON and ERS-1/2. *Journal of Geophysical Research*, 105 (C8), 19477-19498.
- Echevin, V., Crépon, M., Mortier, L., 2003. Simulation and analysis of the mesoscale circulation in the northwestern Mediterranean Sea. *Annales Geophysicae*, 21, 281-297.
- Estrada, M., Varela, R.A., Salat, J., Curzado, A., Arias, E., 1999. Spatio-temporal variability of the winter phytoplankton distribution across the Catalan and north Balearic fronts (NW Mediterranean). *Journal of phytoplankton Research*, 21, 1-20.
- Falkowski, P., Ziemann, D., Kolber, Z., Bienfang, P., 1991. Role of eddy pumping in enhancing primary production in the ocean. *Nature*, 352, 55-58.
- Field, C.B., Behrenfeld, M.J., Randerson, J.T., Falkowski, P., 1998. Primary production of the biosphere: Integrating terrestrial and oceanic components. *Science*, 281 (5374), 237-240.
- Gasparini, G.P., Zodiatis, G., Astraldi, M., Galli, C., Sparnocchia, S., 1999. Winter intermediate water lenses in the Ligurian Sea. *Journal of Marine System*, 20, 319-332.
- Goffart, A., Hecq, J.-H., Legendre, L., 2002. Changes in the development of the winter-spring phytoplankton bloom in the Bay of Calvi (NW Mediterranean) over the last two decades: a response to changing climate? *Marine Ecology Progress Series*, 236, 45-60.
- Grilli, F., Pinardi, N., 1998. The computation of Rossby radii of deformation for the Mediterranean Sea. *MTP News*, 6, 4.
- Hu, Z.Y., Petrenko, A.A., Doglioli, A.M., Dekeyser, I., 2011. Study of a mesoscale anticyclonic eddy in the western part of the Gulf of Lion. *Journal of Marine System*, 88 (1), 3-11.
- Isern-Fontanet, J., Garcia-Ladona, E., Font, J., 2003. Identification of marine eddies from altimetric maps. *Journal of Atmospheric and Oceanic Technology*, 20, 772-778.
- Jenkins, W., 1988. Nitrate flux into the euphotic zone near Bermuda. *Nature*, 331, 521-523.
- Kersalé, M., Petrenko, A.A., Doglioli, A.M., Dekeyser, I., Nencio, F., 2013. Physical characteristics and dynamics of the coastal Latex09 Eddy derived from in situ data and numerical modeling. *Journal of Geophysical Research Oceans*, 118, 399-409.
- Köhl, A., 2007. Generation and stability of a quasi-permanent vortex in the Lofoten Basin. *Journal of Physical Oceanography*, 37, 2637-2651.
- Koszalka, I., Bracco, A., McWilliams, J.C., Provenzale, A., 2009. Dynamics of wind-forced coherent anticyclones in the open ocean. *Journal of Geophysical Research* 114, C08011. doi:10.1029/2009JC005388
- Large, W.G., McWilliams, J.C., Doney, S.C., 1994. Oceanic vertical mixing: a review and a model with a nonlocal boundary layer parameterization. *Reviews of Geophysics*, 32, 363-403.
- Lévy, M., Klein, P., 2004. Does the low frequency variability of mesoscale dynamics explain a part of the phytoplankton and zooplankton spectral variability? *Proceedings of the Royal Society of London A*, 460, 1673-1687.
- Martin, A.P., Richards, K.J., Bracco, A., Provenzale, A., 2002. Patchy productivity in the open ocean. *Global Biogeochemical Cycles*, 16, 1025.
- Marty, J.C., Chiavérini, J., 2010. Hydrological changes in the Ligurian Sea (NW Mediterranean, DYFAMED site) during 1995-2007 and biogeochemical consequences. *Biogeosciences*, 7, 2117-2128.
- Marullo, S., Buongiorno Nardelli, B., Guarracino, M., Santoleri, R., 2007. Observing the Mediterranean Sea from space: 21 years of Pathfinder-AVHRR sea surface temperatures (1985 to 2005): Re-analysis and validation. *Ocean Science*, 3, 299-310.
- Marullo, S., Salusti, E., Viola, A., 1985. Observations of a small-scale baroclinic eddy in the Ligurian Sea. *Deep Sea Research Part A Oceanographic research papers*, 32, 215-222.
- McGillicuddy, D.J., Robinson, A., 1997. Eddy-induced nutrient supply and new production in the Sargasso Sea. *Deep Sea Research Part I*, 44, 1427-1450.
- Millot, C., 1991. Mesoscale and seasonal variabilities of the circulation in the Western Mediterranean. *Dynamics of Atmosphere and Oceans*, 15, 179-214.
- Millot, C., 1999. Circulation in the Western Mediterranean Sea. *Journal of Marine Systems*, 20, 423-442.
- Montani, A., Marsigli, C., Nerozzi, F., Paccagnella, T., Tibaldi, S. et al., 2003. The Soverato flood in Southern Italy: performance of global and limited-area ensemble forecasts. *Nonlinear Processes in Geophysics*, 10, 261-274.
- Nencio, F., Dong, C., Dickey, T., Washburn, L., McWilliams, J., 2010. A vector geometry based eddy detection algorithm and its application to high-resolution numerical model products and high-frequency radar surface velocities in the Southern California Bight. *Journal of Atmospheric and Oceanic Technology*, 27, 564-579.
- Nezlin, N.P., Lacroix, G., Kostianoy, A.G., Djenidi, S., 2004. Remotely sensed seasonal dynamics of phytoplankton in the Ligurian Sea in 1997-1999. *Journal of Geophysical Research*, 109, C07013. doi:10.1029/2000JC000628
- Pascual, A., Faugère, Y., Larnicol, G., Le Traon, P.Y., 2006. Improved description of the ocean mesoscale variability by combining four satellite altimeter missions. *Geophysical*

- Research Letter*, 33, L02611. doi:10.1029/2005GL024633.
- Pasquero, C., Bracco, A., Provenzale, A., 2005. Impact of the spatiotemporal variability of the nutrient flux on primary productivity in the ocean. *Journal of Geophysical Research*, 110, C07005. doi:10.1029/2004JC002738.
- Picco, P., Capelletti, A., Sparnocchia, S., Schiano, M.E., Pensieri, S. *et al.*, 2010. Upper layer current variability in the Central Ligurian Sea. *Ocean Science*, 6, 825-836.
- Poulain, P.-M., Gerin, R., Rixen, M., Zanasca, P., Teixeira, J. *et al.*, 2010. Surface circulation in the Liguro-Provençal basin as measured by satellite-tracked drifters (2007–2009). *OceanDyn.*, submitted for publication. Available from: / <http://www.rsmas.miami.edu/personal/tamay/misc/PMPet2010.pdf>.
- Provenciale, A., 1999. Transport by coherent barotropic vortices. *Annual Review of Fluid Mechanics*, 31, 55-93.
- Rio, M.-H., Hernandez, F., 2004. A Mean Dynamic Topography computed over the world ocean from altimetry, in-situ measurements and a geoid model. *Journal of Geophysical Research*, 109, 12.
- Robinson, A.R., Leslie, W., Theocharis, A., Lascaratos, A., 2001. *Mediterranean Sea circulation*. p. 1689- 1705. In: *Ocean Currents*. Encyclopedia of Ocean Science, vol. 3. Academic Press, San Diego, CA.
- Sadarjoen, A., Post, F.H., 2000. Detection, quantification, and tracking of vortices using streamline geometry. *Visualization and Computer Graphics*, 24, 333-341.
- Sammari, C., Millot, C., Prieur, L., 1995. Aspects of the seasonal and mesoscale variabilities of the Northern Current in the western Mediterranean Sea inferred from the PROLIG-2 and PROS-6 experiments. *Deep-Sea Research*, 42 (6), 893-917.
- Santoleri, R., Salusti, E., Stocchino, C., 1983. Hydrological currents in the Ligurian Sea. *Il Nuovo Cimento C*, 6, 353–370.
- Schroeder, K., Millot, C., Bengara, L., Ben Ismail, B., Bensi, M., *et al.*, 2012. Long-term monitoring programme of the hydrological variability in the Mediterranean Sea: a first overview of the HYDROCHANGES network. *Ocean Science Discussion*, 9, 1741-1812.
- Shchepetkin, A.F., McWilliams, J.C., 2003. A method for computing horizontal pressure-gradient force in an oceanic model with a nonaligned vertical coordinate. *Journal of Geophysical Research*, 108 (C3), 3090. doi:10.1029/2001JC001047.
- Shchepetkin, A.F., McWilliams, J.C., 2005. The regional ocean modeling system: a split-explicit, free-surface, topography following coordinates ocean model. *Ocean Modelling*, 9, 347-404.
- Steppeler, J., Doms, G., Schättler, U., Bitzer, H.W., Gassmann, A. *et al.*, 2003. Mesogamma scale forecast using the nonhydrostatic model LM. *Meteorology and Atmospheric Physics*, 82, 75-96.
- Troupin, C., Sangrà, P., Aristegui, J., 2010. Seasonal variability of the oceanic upper layer and its modulation of biological cycles in the canary island region. *Journal of Marine Systems*, 80, 172-183.